Comparison of numerical schemes for the bidomain model

Y. Bourgault*, M. Ethier

Department of Mathematics and Statistics, University of Ottawa On, Canada K1N 6N5

Abstract

Bidomain models become increasingly popular for studying and simulating electrophysiological waves in the cardiac tissue. We study and compare different numerical schemes to solve the bidomain equations. Our analysis is based on criteria such as the stability and accuracy of the schemes.

Keywords: Anisotropic bidomain models; Electrophysiology; Numerical schemes

1. Introduction

Bidomain models have become increasingly popular for simulating electrophysiological waves in the cardiac tissue (see [1,2] and references therein). Being rather complex nonlinear models they benefit from the use of sophisticated solution methods and, because of this, the focus of the research in the domain has moved over the years to the application of finite volume and finite element solvers over unstructured meshes [3,4]. Researchers also started to investigate the use of implicit and semi-implicit time-stepping methods to solve bidomain models [5,6].

In [7], we proposed a fully implicit linear finite element method working on unstructured meshes composed of triangles and tetrahedra for solving an anisotropic bidomain model. The capabilities of the method in computing 2-D and 3-D re-entrant waves were demonstrated on arbitrary meshes and, in the 2-D case, some results were illustrating the numerical requirements of the method to ensure an accurate simulation of the dynamics of spiral wave tips. The implicit finite element method proposed in that paper did not suffer from strict stability requirements but, on the other hand, its efficiency in term of CPU time requirements turned out to be critically dependent on the development of fast preconditioned iterative solvers. This paper continues the work done in [5] by testing different time-stepping methods, while at the same time offering a theoretical analysis of the methods' stability and convergence to the exact solution.

* Corresponding author. Tel.: +1 613 562 5800; Fax: +1 613 562 5776; E-mail: ybourg@mathstat.uottawa.ca

Computational Fluid and Solid Mechanics 2005
K.J. Bathe (Editor)

In the next section, we present the bidomain model with FitzHugh–Nagumo kinetics behind our simulations and analyses. In Section 3, the different numerical schemes are presented. In the last section, we show some numerical results, including the error associated to our most important methods.

2. General anisotropic bidomain model

Different formulations of the bidomain equations are available. For our analyses and simulations, we assumed that no source current was applied to the system, which allowed us to write the system as follows:

$$\frac{\partial u}{\partial t} = \frac{1}{\epsilon} f(u,v) + \nabla \cdot (\sigma_i \nabla u) + \nabla \cdot (\sigma_i \nabla u_e) \tag{1}$$

$$\nabla \cdot (\sigma_i \nabla u + (\sigma_i + \sigma_e) \nabla u_e) = 0 \tag{2}$$

where u_e is the extra-cellular potential, u is the transmembrane potential, and σ_i and σ_e are the intra- and extra-cellular conductivity tensors, respectively. The ion activity may be represented using idealized FitzHugh–Nagumo kinetics, which adds an ordinary differential equation for the 'ion concentration' v:

$$\frac{\partial v}{\partial t} = \epsilon g(u,v) \tag{3}$$

where $g(u, v) = u + \beta - \gamma v$ and ϵ, β and γ are parameters controlling the ion kinetics. This extra ODE is coupled with the bidomain model by means of the function

$$f(u,v) = u - \frac{u^3}{3} - v \tag{4}$$

We should also note that in the 1-D case, the bidomain equations reduce to the so-called 'monodomain formulation'. In this case, the two PDEs may reduce to a single equation:

$$\frac{\partial u}{\partial t} = \frac{1}{\epsilon} f(u,v) + \frac{\partial}{\partial x}\left(\frac{\lambda(x)}{1+\lambda(x)}\sigma_i(x)\frac{\partial u}{\partial x}\right) + c(t)\frac{\partial}{\partial x}\left(\frac{1}{1+\lambda(x)}\right) \tag{5}$$

where $\lambda(x) = \frac{\sigma_e(x)}{\sigma_i(x)}$. In the case where $\lambda(x)$ is a constant function, the last term of Eq. (5) disappears.

3. Methods and analysis

We solved the Eqs (1)–(3) in 1-D using several numerical schemes with finite difference and finite element methods for the space discretization. Here, only the finite difference results are shown, as the finite element solutions have the same behaviour.

Suppose that A_i and A_e are respectively finite difference approximations for the operators $-\frac{\partial}{\partial x}(\sigma_i\frac{\partial}{\partial x})$ and $-\frac{\partial}{\partial x}(\sigma_e\frac{\partial}{\partial x})$. For Eq. (1), we used the θ-method, which writes as

$$\frac{u^{n+1}-u^n}{\Delta t} = \frac{1}{\epsilon} f(u^n,v^n) - A_i((1-\theta)(u^n+u_e^n) + \theta(u^{n+1}+u_e^{n+1})) \tag{6}$$

with some values of θ, namely $\theta = 0$ (explicit Euler) and $\theta = \frac{1}{2}$ (Crank–Nicolson). We also tried the semi-implicit second-order Gear scheme

$$\frac{\frac{3}{2}u^{n+1} - 2u^n + \frac{1}{2}u^{n-1}}{\Delta t} = \frac{1}{\epsilon} f(u^n,v^n) - A_i(u^{n+1}+u_e^{n+1}) \tag{7}$$

and the completely implicit Euler method

$$\frac{u^{n+1}-u^n}{\Delta t} = \frac{1}{\epsilon} f(u^{n+1},v^{n+1}) - A_i(u^{n+1}+u_e^{n+1}) \tag{8}$$

Eq. (2) is always solved in an implicit way:

$$A_i u^{n+1} + (A_i + A_e)u_e^{n+1} = 0 \tag{9}$$

which must be solved simultaneously to Eqs (6), (7) or (8) unless we use the θ-method with $\theta = 0$. Then, we typically solve Eq. (3) with an explicit Euler or Gear scheme, unless the completely implicit Euler method is used, in which case it is solved simultaneously to the other equations with an implicit Euler scheme.

We also obtained analytical stability results for some of the numerical schemes.

Proposition 3.1 Let u^m and v^m be computed with the fully implicit Euler scheme (8) for the bidomain model with the FitzHugh–Nagumo cell model. For any $\Delta t < \frac{\delta\epsilon}{3}$ with $\delta \in]0, 1[$,

$$\|u^m\|_0^2 + \|v^m\|_0^2 \le \frac{e^{\frac{3T}{\epsilon(1-\delta)}}}{1-\delta}\left[\|u^0\|_0^2 + \|v^0\|_0^2 + T\epsilon\beta^2 mes(\Omega)\right] \tag{10}$$

for $m = 0, 1, \ldots, N$, $N\,\Delta t = T$, where T is the time at the last iteration, $\|\cdot\|_0$ denotes the L^2-norm on the space domain and $mes(\Omega)$ denotes the size of the space domain. Moreover,

$$C(\|u\|_{L^2(0,T;H^1)} + \|u_e\|_{L^2(0,T;H^1)}) \le \|u^0\|_0^2 + \|v^0\|_0^2 + T\varepsilon\beta^2 mes(\Omega) + \frac{3}{\epsilon}(\|u\|_{L^2(0,T;L^2)} + \|v\|_{L^2(0,T;L^2)})$$

for some positive constant C.

Proposition 3.2 Suppose that we compute u^m with the θ-scheme (6) with $\theta = 0$ (explicit Euler) using any ion dynamics. Then, to ensure stability of u^m, the following condition must be satisfied:

$$\Delta t = O\left(\frac{h^2 m^2}{M^4}\right) \tag{11}$$

where h is the size of the space element and the eigenvalues of the tensors σ_i and σ_e lie in the interval $[m, M]$. As well, if we compute v^m with the explicit Euler method, to ensure stability, Δt must satisfy

$$\Delta t(L_f/\epsilon + \epsilon L_g) < 2 \tag{12}$$

where L_f and L_g are respectively the Lipschitz constants of f and g.

4. Numerical results

We solve the bidomain equations in 1-D in the case of equal conductivities $\sigma_i = \sigma_e = 1.0$ with parameters $\beta = 1.0$, $\gamma = 0.5$ and $\epsilon = 0.1$. The domain used is the interval [0, 70] in space and [0, 40] in time. For an initial condition, we use constant solutions at the equilibrium values for u, u_e and v, except that we already excite u on the interval [0, 3.5]. This gives a pulse wave that propagates along the length of the domain.

Since we cannot get an exact solution of the bidomain equations we use, as a reference, a numerical solution obtained with the semi-implicit Gear scheme, with 8000 space elements and 50 000 time steps. This solution has been validated with another precise solution, and it is therefore precise enough to be used as an 'exact' solution. See Fig. 1 for an image of the solution at different times.

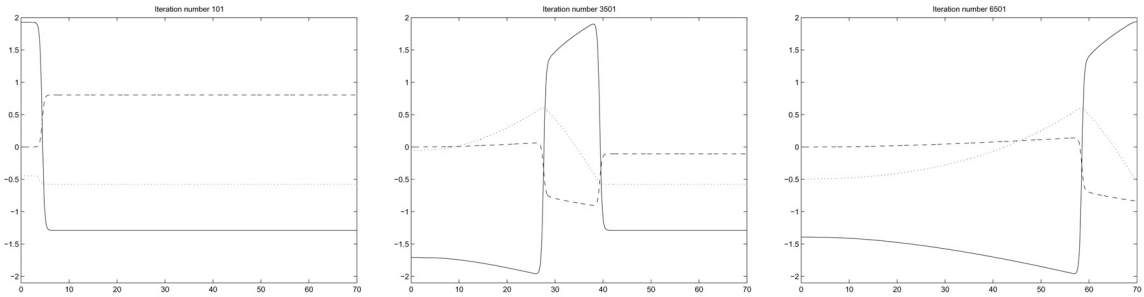

Fig. 1. 'Exact' solution to the bidomain equations at several times t. u: continued line, u_e: dashed line, v: dotted line.

Table 1
Numerical and theoretical critical time-steps

	Numerical		Theoretical	
Methods	$N = 500$	$N = 1000$	$N = 500$	$N = 1000$
Explicit Euler	0.0083–0.0095	0.0023–0.0024	0.001109	0.000277
Crank–Nicolson	0.0444–0.1142	0.0229–0.1	0.05	0.05
Implicit Euler	> 0.2	> 0.2	0.0333	0.0333
Semi-implicit Gear	0.0667–0.16	0.0667–0.16		

Table 1 shows the theoretical and numerical stability limits for several values of the number N of space elements. Note that the nonlinearity of Eq. (1) makes the experimental critical time-step difficult to pinpoint, since an instability may appear, then be 'smoothened out' after a number of time-steps, preventing the solution from exploding. We have, therefore, given a critical stability interval instead of a precise value. The smallest value is the necessary time-step to ensure that no instability appears while the largest is the necessary time-step to ensure that the solution will remain bounded. The theoretical values for the critical time-step follow from the estimates (10)–(12), evaluating all constants involved for the 1-D problem.

For the convergence tests, our main result was that the explicit Euler method appears to be the most appropriate to this particular problem. Despite its very strict stability requirements, even with a time step that is not much smaller than the experimental stability limit, we reach a degree of accuracy that is not equalled by any other method we tried, even when we take a time-step as small as the one we used for explicit Euler. This is an unexpected result, as Crank–Nicolson is accurate to second order in time while explicit Euler is only accurate to first order in time. Figure 2 shows the evolution of the L^2-error of u as a function of time for our four methods, with 1000 grid points. The error for the implicit Euler method is shown for a test done with 500 time-steps instead of 20 000, because the computational resources that would have been required to do 20 000 time-steps with this method would have been prohibitive. The L^∞-error is not shown here but has a behaviour similar to the L^2-error. We note that often the error sees a peak soon after $t = 0$ and again at $t = 26$ and $t = 30$. The first peak may be due to the fact that the wave takes a few iterations to settle in its correct form, depending on the method used, and the last two peaks appear because the wave leaves the domain and may suffer the influence of the boundary.

To conclude, while the semi-implicit Gear method is the most stable of all explicit and semi-implicit methods we tried, it does not seem to offer any substantial advantage when it comes to the exactness of the numerical solution. In fact, it seems that the explicit Euler method yields the most exact solution, probably because the speed of the pulse wave computed numerically with explicit Euler converges faster to the actual speed of the pulse wave. Proving this fact will be a future orientation of our research. We are also currently working on finding a theoretical stability limit for the semi-implicit Gear method, which should not depend on N, and in the process of doing 3-D simulations using the bidomain model. Given that we already have experience with the 3-D bidomain model (see [7]), it should be easy

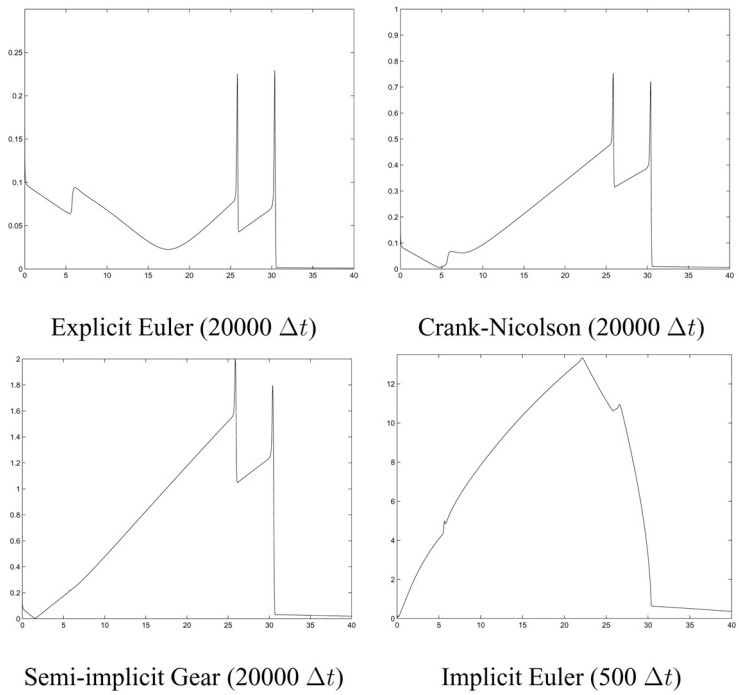

Fig. 2. L^2-norm of the error on u between different approximations with 1000 grid points and the 'exact' solution, with respect to time.

to apply the knowledge gained here to this other problem.

Acknowledgements

The authors would like to thank NSERC for an operating grant and a scholarship under which this work was supported. The authors are also thankful to Prof. Yves Coudière from the Université de Nantes for fruitful discussions during the course of this work.

References

[1] Panfilov AV, Holden AV, editors. Computational Biology of the Heart. John Wiley & Sons, 1997.
[2] Keener J, Sneyd J. Mathematical Physiology. Springer-Verlag, 1998.
[3] Harrild DM, Henriquez CS. A finite volume model of cardiac propagation. Annals Biomed Eng 1997;25:315–334.
[4] Rogers J, Courtemanche M, McCulloch A. Finite element methods for modelling impulse propagation in the heart in: AV Panfilov, AV Holden, editors, Computational Biology of the Heart, pp. 217–233. John Wiley & Sons, 1997.
[5] Keener JP, Bogar K. A numerical method for the solution of the bidomain equations in cardiac tissue. Chaos 1998;8:234–241.
[6] Murillo M, Cai XC. Parallel Newton–Krylov–Schwarz method for solving the anisotropic bidomain equations from the excitation of the heart model. Lecture Notes in Computer Science 2002;2329:533–542.
[7] Ethier M, Bourgault Y, LeBlanc VG. Simulation of electrophysiological waves with an unstructured finite element method. ESAIM: Mathematical Modelling and Numerical Analysis 2003;37:649–661.